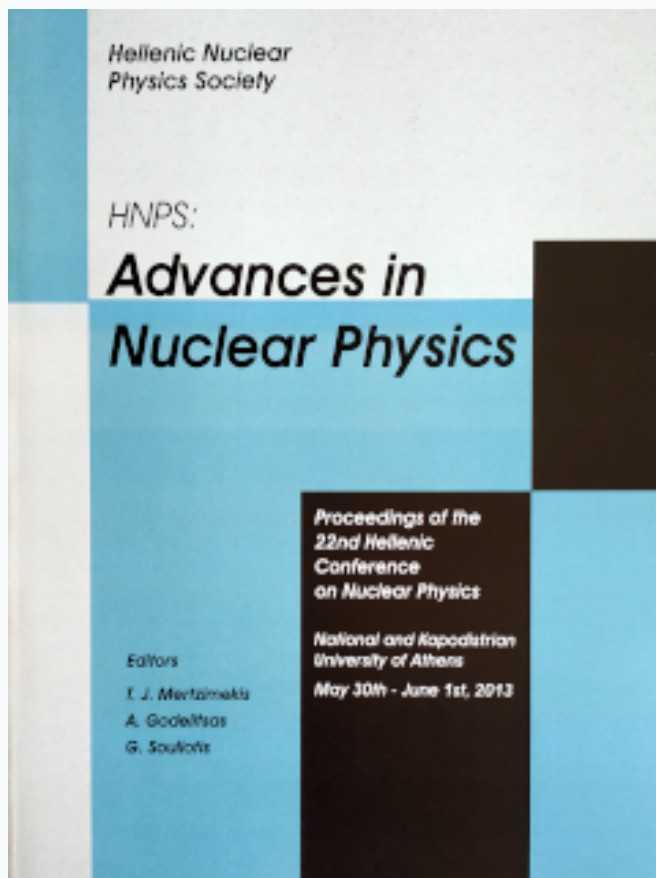


HNPS Advances in Nuclear Physics

Vol 21 (2013)

HNPS2013



High energy fission cross sections induced by deuteron on ^{232}Th and proton on natPb targets

M. Zamani, S. Stoulos, M. Fragopoulou, M. Krivopustov

doi: [10.12681/hnps.2014](https://doi.org/10.12681/hnps.2014)

To cite this article:

Zamani, M., Stoulos, S., Fragopoulou, M., & Krivopustov, M. (2019). High energy fission cross sections induced by deuteron on ^{232}Th and proton on natPb targets. *HNPS Advances in Nuclear Physics*, 21, 116–122.

<https://doi.org/10.12681/hnps.2014>

High energy fission cross sections induced by deuteron on ^{232}Th and proton on ^{nat}Pb targets

M. Zamani^a, S. Stoulos^a, M. Fragopoulou^a, M. Krivopustov^b

^a*Aristotle University of Thessaloniki, School of Physics, Thessaloniki, 54124, Greece*

^b*Joint Institute for Nuclear Research, Dubna, 141980, Russia*

Abstract

Total fission cross sections induced by deuterons with energies 1.6, 2.5 and 4.0 GeV on ^{232}Th targets and by protons on ^{nat}Pb targets at energy 2.0 GeV were measured during irradiations at the Nuclotron accelerator, JINR, Dubna. Using Solid State Nuclear Track detectors, the fission cross sections induced by deuterons on ^{232}Th were determined as 1277 ± 216 , 1232 ± 207 and 1153 ± 198 mb, corresponding to the energies mentioned above. The total fission cross section of protons on ^{nat}Pb was estimated by the same method as 131 ± 30 mb. These results were compared to the previous systematic parameterization of proton induced fission and new values for the parameters of deuteron-induced fission on actinides, ^{232}Th and ^{238}U and proton induced fission on ^{nat}Pb were deduced. Fitting results obtained for deuterons on actinides are discussed and compared to results for protons.

Keywords: fission, total cross section, ^{232}Th , ^{nat}Pb

PACS: 25.85.Ge, 25.45.-z, 25.40.Sc

1. Introduction

Fission induced by light particles at high energies is quite different from the low energy process. Studies on low energy fission involve reactions that proceed through the stage of compound nucleus formation due to fusion of the projectile with the target [1]. In this case, the fissioning nucleus is well defined and has definite excitation energy. The cross section for fusion diminishes and may even vanish at projectile energies higher than 50-100 MeV/nucleon [2]. The fission process at low incident energies is about equal to the reaction cross section, since the direct process cross section is a small fraction of the reaction cross section and pre-equilibrium processes are improbable. As the projectile energy increases, the compound nucleus formation cross section becomes progressively smaller than the reaction cross section, due mainly to the increased probability of particle emission. Fission induced by high energy particles is described as a two-step process: collisions induce the rapid formation of an excited prefragment, which de-excites by particle emission and/or fission [3, 4]. In heavy compound nuclei, fission is a competing decay mode to other mechanisms, especially if the compound nucleus formed has a high angular momentum. Therefore, the compound nucleus cross section is the sum of the cross sections corresponding either to evaporation residues or to pairs of fission fragments. The high energy part of fission cross sections represents the energy region in which the compound nucleus formation is restricted while more rapid processes like fragmentation reactions take place considering that at high energies inelastic cross sections remain stable with increasing energy. Fission studies at intermediate and high energies are of high interest for the research of the reaction mechanisms, because fission can be produced directly by the projectile-target interaction at both large and small impact parameters, but also because it can be the ending effect of spallation reactions.

In the evolution of fission studies, which is connected to the history of accelerator energies and facilities in the transition region, 70-1000 MeV, the fission cross section data and their evaluation are missing from the literature, especially for light projectiles, heavier than protons. Most of the data in the literature refer to fission induced by protons, such as in the extended report of proton induced reactions by Hufner [5]. Viola's

systematics [6] also includes fission cross section data in a wide range of proton energies. The experimental data of proton induced fission cross sections for sub-actinides like ^{nat}Pb and ^{209}Bi , in the energy range below 1 GeV, were reproduced by calculation and the systematic of fission cross sections has been derived [7].

A multitude of data on fission mechanism has been presented concerning deuterons and especially alpha particles as projectiles, but mostly at low energies [8–14]. Limited results are published on fission as a parallel product of high energy reaction mechanism, i.e. spallation-fission. Some of those studies [3, 4, 15, 16], referring to proton and deuteron induced spallation/fission, underline the different origin of fission at lower energies. In recent years, due to the applications in Accelerator Driven Systems, fission research has been extended to higher energies, at GeVs. However, limited experimental data have been presented in the literature regarding deuteron projectiles [17–19] and even less for alpha particles [20], although they are very useful for the comparison of the experimental data to both statistical and dynamical models of fission [2]. Some of those results, referring to high energy deuterons on actinide and sub-actinide targets [17, 19] were obtained during experiments at the NUCLOTRON accelerator; JINR, Dubna, in the frame of the international collaboration “Energy plus Transmutation” [21].

2. Experimental Procedure

In the present study the total fission cross section of ^{232}Th due to deuteron beams of 1.6 and 2.5 GeV was determined, as a continuation of previous work [19] referring to 4 GeV deuteron beam induced fission on actinides (^{238}U , ^{235}U , ^{232}Th) and sub-actinides (^{209}Bi , ^{197}Au). In addition, the total fission cross section of ^{nat}Pb induced by 2 GeV protons was estimated by evaluating previous irradiation data. Cross section determination was achieved using fissionable targets, manufactured in the CNRS; Strasbourg, France, by evaporation on Lexan foils [22]. Lexan sheets were used also for the detection of fission fragments. The mass of ^{232}Th targets was measured using alpha and gamma ray spectrometry at the Laboratory of Nuclear Physics of the Aristotle University of Thessaloniki, Greece, while the mass of ^{nat}Pb was given by the manufactures. A detailed analysis of the instrumentation and method applied has been presented in a previous publication [19]. A representation of the fission fragments with the detection system can be shown in Fig. 1. The method of experiment provides an event by event analysis. The measured track lengths correspond to the range of fission fragments in the detector (under the condition that tracks are fully developed). The angles of the fragments relative to the beam direction (δ_1, δ_2) were determined by measuring the depth of the track and the track length. The projection of the tracks to the layer perpendicular to the beam (upper detector surface) gives the angles between fission fragments and provides a test of the equilibration of momentum in each individual event [10, 11, 22].

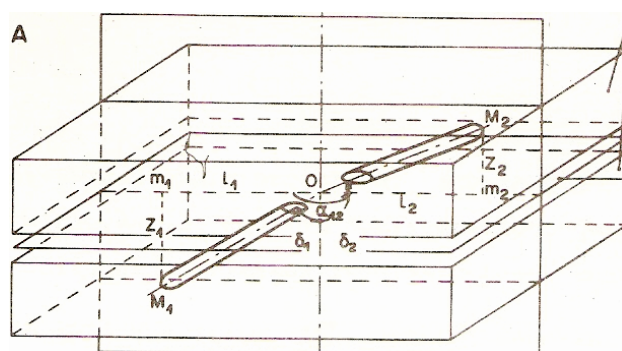


Figure 1: Representation of the experimental set up with upper and lower detectors (4π geometry). The fission fragments are visible under an optical microscope. The track characteristics under measurement are indicated.

3. Results and Discussion

The total fission cross section data, obtained using the experimental set up described in detail in Ref. [19], is presented in Table 3. The fission cross section as a function of proton energy depends on four parameters of different physical meanings according to the evaluation performed for proton induced fission on sub-actinides in the medium energy region, using calculation codes [7]. An equation describing the systematic of fission cross section and reproduce the experimental data in good agreement at energies below 1 GeV is the following [7]:

$$S = P_1 [1 - \exp[-P_2(E_p - P_3)]] \quad (1)$$

where P_1 is the fission “saturation cross section” corresponding to the maximum of the cross section systematic; P_2 is the fission “saturation constant”, describing the increasing rate of the fission cross section with energy up to a maximum value and P_3 is the “apparent energy threshold” for the projectile-target system studied. An extension to higher proton energies was provided for actinides and for sub-actinides as well in Ref. [23]. The improved systematic introduces an additional fitting parameter P_4 to equation 1 in order to reproduce the decrease of the fission cross sections at high energies. The new formula is given now as:

$$S_{new} = S(1 - P_4 \ln E_P) \quad (2)$$

The parameter P_4 , named by us as the “fission decrease constant” depends on the projectile-target system. The decrease of the fission cross sections at intermediate and high energies are attributed to the increase of more violent processes than fission as the energy of the projectile increases [5].

Energy [GeV]	^{nat}Pb (p,f)	^{232}Th (d,f)
2.0	131 ± 30	
1.6		1277 ± 216
2.5		1232 ± 207
4.0		1153 ± 198

Table 1: Total fission cross section data

This fitting describes successfully the fission cross sections behavior versus proton energy, especially for actinides. In the case of sub-actinides, there are contradictory results in the literature, depending on the experimental data selected [23]. Proton-induced fission on ^{nat}Pb targets presents an unclear situation as to whether the cross sections continue to be stable or present a decrease (Fig. 2). A saturation of fission cross sections with energy at intermediate and high range has been presented according to the data published after 2001 [24]. The total fission cross section at 2 GeV protons on ^{nat}Pb estimated in the present work matches the experimental data of earlier publications [22, 24, 25]. Taken into account all available data on proton-induced fission on ^{nat}Pb presented up to today [22, 24–28] saturation can be accepted for total fission cross section at high energies. Therefore, we performed the same fitting process including the recent and our experimental results for ^{nat}Pb using equations 1 and 2. Both equations reproduce well the experimental data (Table 3), with equation 2 appearing to be more successful than equation 1. The necessity of additional experimental data, especially at high energies, is apparent in order to clarify the behavior of ^{nat}Pb fission process at that energy range.

Typical fitting curves of fission cross sections are given in Figs. 3 as a function of proton energy for ^{232}Th and ^{238}U , according to the results presented in Ref. [23]. The general observation in figs. 3 is the similar behavior of fission cross sections as a function of projectile energy independently of the projectile type. Both curves present an increase at low energies which continues up to a maximum. After this point, heavy nuclei such as actinides present a decreasing cross section with projectile energy. Assuming that both actinide isotopes follow the same pattern of fission process as has been demonstrated by proton-induced fission, fitting parameters can be calculated using the available data on deuteron induced fission. Taken under consideration the available data of ^{238}U at low energies (< 100 MeV/nucleon) the fitting process can

	Using Eq. 2 $R^2 = 92\%$	Using Eq. 1 $R^2 = 89\%$
saturation cross section, P_1 [mb]	198 ± 24	134 ± 9
saturation constant, $P_2 \times 10^{-3}$ [MeV $^{-1}$]	4.2 ± 0.7	6.3 ± 0.9
apparent threshold energy, P_3 [MeV]	58 ± 13	62 ± 13
fission decrease constant, $P_4 \times 10^{-3}$ [MeV $^{-1}$]	40 ± 9	—

Table 2: Fitting parameters determined on proton-induced fission cross section data of ^{nat}Pb

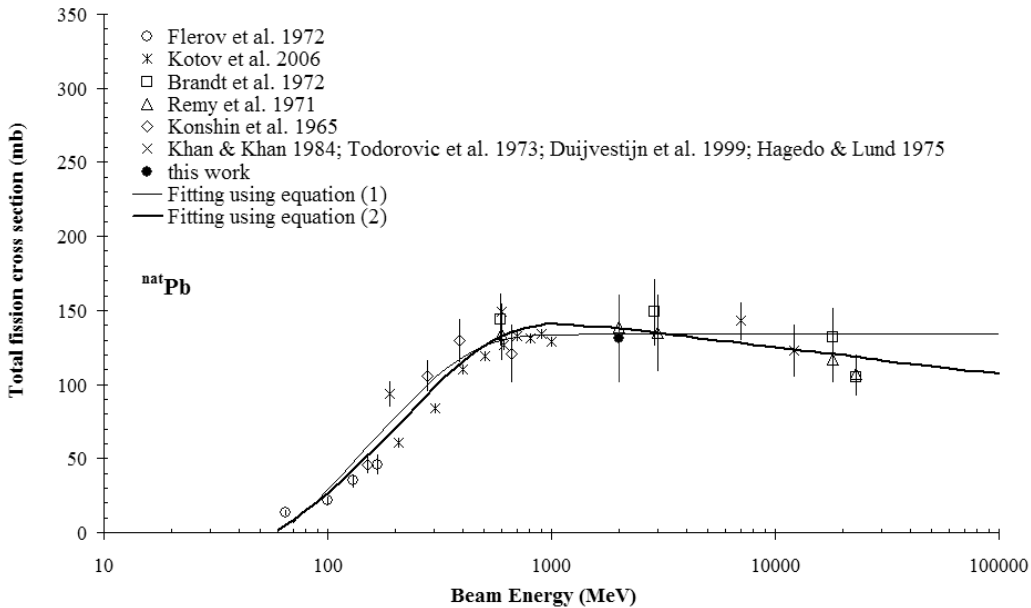


Figure 2: Proton induced fission cross section on ^{nat}Pb . The solid curves represent the fitting according to the parameters given in Table 2.

be applied using equation 2 in order to estimate the parameters P_2 and P_3 , which can not be calculated using ^{232}Th fission cross section, since there are limited experimental data at low energies. The contribution of the specific work on ^{232}Th fission at high energies permits the calculation of parameter P_4 by fitting equation 1 on ^{232}Th data, taking into account the parameters estimated from data on ^{238}U . The parameters deduced by the fitting with deuteron projectiles have a better correlation for ^{238}U ($= 90\%$) than ^{232}Th ($= 70\%$) and are presented in Table 3. In the same table the parameters produced by the new fitting for deuterons are compared to the ones for protons [23].

In the fittings performed each calculated fitting parameter in the following is examined separately. The fission “saturation cross section” P_1 , representing the maximum of the fission cross section, is estimated for deuteron with ^{232}Th interaction as 2.57 ± 0.39 b. This value is 1.47 ± 0.22 times higher than the proton’s one. The same conclusion arises from the ^{238}U saturation cross section (3.78 ± 0.38 b) which is 1.60 ± 0.16 times higher than the corresponding proton cross section. Similar ratios are observed comparing the fission cross section data available in the literature [8–10, 24–28] for protons and deuterons at the same energy ranges. The deuteron fission cross section is 1.36 to 1.69 times higher than in the case of protons for energies around 100 MeV while for energies at the GeVs range the deuteron fission cross section is reduced, varying between 1.03 and 1.24 times the proton cross sections. This result could be connected to the difference observed in neutron multiplicities when massive spallation targets, such as Bi, Pb, Th, U irradiated with

	^{232}Th		^{238}U	
	p	d	p	d
saturation cross section, P_1 [mb]	1750	2572 ± 392	2360	3781 ± 379
saturation constant, $P_2 \times 10^{-3}$ [MeV^{-1}]	111	41 ± 17	111	38 ± 11
apparent threshold energy, P_3 [MeV]	12.1	24.3 ± 9.4	12.1	24.3 ± 9.4
fission decrease constant, $P_4 \times 10^{-3}$ [MeV^{-1}]	67	70 ± 9	67	73 ± 8

Table 3: Fitting parameters determined on deuteron-induced fission cross section data on actinides. The data of proton-induced fission are from Ref. [23].

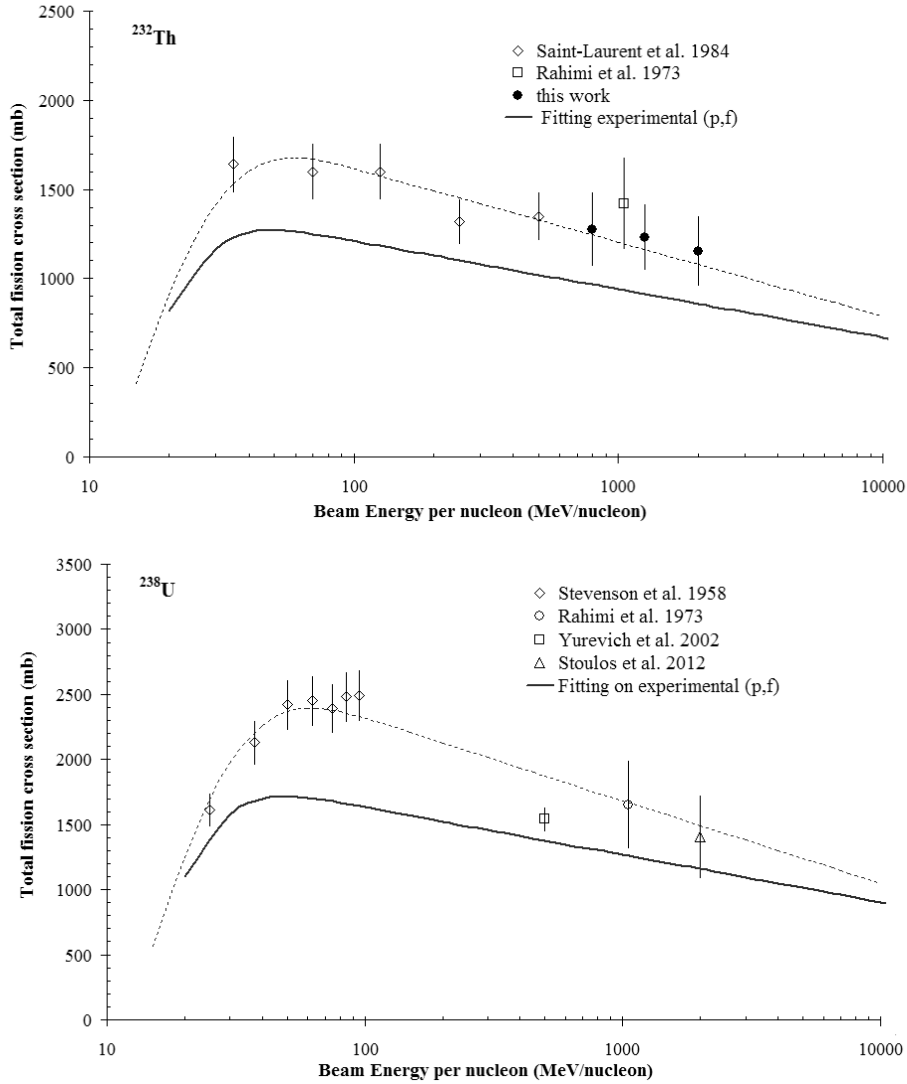


Figure 3: Deuteron induced fission cross section on ^{232}Th (a-top) and ^{238}U (b-bottom). The solid lines represent the fitting of proton data [23] while the dashed lines of deuteron data, according to the parameters given in Table 3

deuteron beams at the GeVs range [29, 30]. The “fission saturation constant”, P_2 , of ^{232}Th and ^{238}U for deuterons is about one third relative to protons. Therefore, the maximum of the fission cross section induced by deuterons is shifted towards higher energy (≈ 20 MeV/nucleon) relative to protons, for which the maximum appears around 50 MeV. The “apparent energy threshold”, P_3 , of deuterons was estimated to be twice the corresponding to protons as a result of the double mass of deuterons relative to protons. Both proton and deuteron fitting results estimate an “apparent energy threshold”, of ≈ 12 MeV/nucleon. The “fission decrease constant”, P_4 , of deuteron curves estimated for both actinides (^{232}Th and ^{238}U) appears to be similar to the “fission decrease constant” of protons, within the fitting uncertainties. However, the fitting parameter P_4 , at these energies, is based on very limited experimental data available in the literature for deuteron-induced fission on actinides, especially for ^{238}U . The sub-actinides fission cross section data are of special interest in order to investigate the decrease of fission processes with increasing energy since the available proton data are either limited or/and contradictory. Further fission studies at intermediate-high energies using light particles are necessary, since the fission cross section drop provides valuable information regarding the competition between fission and other mechanisms at high energies.

4. Conclusions

The fission “saturation cross section” P_1 , representing the maximum of the fission cross section, is estimated for deuteron with ^{232}Th interaction as 2.57 ± 0.39 b. This value is 1.47 ± 0.22 times higher than the proton’s one. The same conclusion arises from the ^{238}U saturation cross section (3.78 ± 0.38 b) which is 1.60 ± 0.16 times higher than the corresponding proton cross section. The deuteron fission cross section is 1.36 to 1.69 times higher than in the case of protons for energies around 100 MeV while for energies at the GeVs range the deuteron fission cross section is reduced, varying between 1.03 and 1.24 times the proton cross sections. This result could be connected to the difference observed in neutron multiplicities when massive spallation targets, such as Bi, Pb, Th, U irradiated with deuteron beams at the GeVs range.

The “fission saturation constant”, P_2 , of ^{232}Th and ^{238}U for deuterons is about one third relative to protons. Therefore, the maximum of the fission cross section induced by deuterons is shifted towards higher energy (≈ 20 MeV/nucleon) relative to protons, for which the maximum appears around 50 MeV.

The “apparent energy threshold”, P_3 , of deuterons was estimated to be twice the corresponding to protons as a result of the double mass of deuterons relative to protons. Both proton and deuteron fitting results estimate an “apparent energy threshold”, of ≈ 12 MeV/nucleon. The “fission decrease constant”, P_4 , of deuteron curves estimated for both actinides (^{232}Th and ^{238}U) appears to be similar to the “fission decrease constant” of protons, within the fitting uncertainties. However, the fitting parameter P_4 , at these energies, is based on very limited experimental data available in the literature for deuteron-induced fission on actinides, especially for ^{238}U .

Sub-actinides fission cross section data are of special interest in order to investigate the decrease of fission processes with increasing energy since the available proton data are either limited or/and contradictory. The results of the present work [31] present the interest for further fission studies at intermediate-high energies using light particles, since the fission cross section behavior versus projectile energy provides valuable information regarding the competition between fission and other mechanisms at high energies.

References

- [1] R. Vandenbosch and J. Huizenga, Nuclear Fission (Academic Press, New York, 1973).
- [2] A. J. Cole, Statistical Models for Nuclear Decay (IOP Publishing Ltd, 2000);
- [3] J. Cugnon, C. Volant, and S. Vuillier, Nucl.Phys. A 625, 729 (1997).
- [4] T. Enqvist, et al., Nucl.Phys. A 703, 435 (2002).
- [5] J. Hufner, Phys. Reports 125, 129 (1985).
- [6] V. E. Viola, B.B. Back, K. L. Wolf, T. C. Awes, C. K. Gelbke, H. Breuer, Phys. Rev. 26, 178 (1982) ; V. E. Viola, K. Kwiatkowski, and M. Walker, Phys. Rev. C 31, 1550 (1985).
- [7] T. Fukahori, and S. Pearlstein, IAEA Report INDC (NDS)-245, 1991, p.93.
- [8] F. Saint Laurent, M. Conjeaud, R. Dayras, S. Harar, H. Oeschler, and C. Volant, Nucl. Phys. A 422, 307 (1984).
- [9] P. Stevenson, H. Hicks, W. Nervik, and D. Nethaway, Phys. Rev. 111, 886 (1958).
- [10] F. Rahimi, D. Cheysari, G. Remy, J. Tripier, J. Ralarosy, R. Stein, and M. Debeauvais, Phys. Rev. C 8, 1500 (1973).

- [11] J. Ralarosy, M. Debeauvais, G. Remy, J. Tripier, R. Stein, D. Buss, Phys. Rev. C 8, 2372 (1973); M. Debeauvais, and J. Tripier, Nucl. Instr. Methods 173, 157 (1980).
- [12] B. Grabez, Z. Todorovic, and R. Antanasijevic, Nucl. Instr. Methods 147, 267 (1977).; W. G. Meyer, H. H. Gutbrod, Ch. Lukner, and A. Sandoval, Phys. Rev. C 22, 179 (1980).
- [13] V.E. Viola, and T. Sikkeland, Phys. Rev. 128, 767 (1962); H. Hicks, et al., Phys. Rev. 128, 700 (1962); G.P. Ford, and R.B. Leachman, Phys. Rev. 137, B826 (1965).
- [14] J. Gindler, et al., Nucl. Phys. A 145, 337 (1970); N.I. Zaika, et al., Soviet Jr. Nuclear Physics 31, 22 (1976); Skobelev, et al., Radiat. Measur. 25, 267 (1995).
- [15] E. Casarejos, et al., Phys. Rev. C 74, 044612 (2006).
- [16] J. Benlliure, P. Armbruster, M. Bernas, A. Boudard, T. Enqvist, R. Legrain, S. Leray, F. Rejmund, K.-H. Schmidt, C. Stphan, L. Tassan-Got, C. Volant, Nucl. Phys. A 700, 469 (2002).
- [17] V. Sotnikov, et al., in 3rd Int. Conf. Cur. Prob. in Nucl. Phys. Atom. Ene., Kyiv, 2010, p.250. <http://www.kinr.kiev.ua/NPAE-Kyiv2010/html/Proceedings/2/sotnikov.pdf>.
- [18] V. Yurevich, V. Nikolaev, R. Yakovlev, and A. Sosnin, Phys. At. Nucl. 65, 1383 (2002).
- [19] S. Stoulos, W. Westmeier, R. Hashemi-Nezhad, M. Fragopoulou, A. Lagoyannis, and M. Zamani, Phys. Rev. C 85 024612 (2012).
- [20] M. Trotta, et al., Phys. Rev. Let. 84, 2342 (2000); Y.E. Penionzkevich, et al., Europ. Phys. Journal A 13, 123 (2002); A.A. Hassan et al., Jour. Bull.Russian Academy of Sciences 70, 1785, (2006).
- [21] M. Krivopustov, et al., Kerntechnik 68, 48 (2003).
- [22] G. Remy, J. Ralarosy, R. Stein, M. Debeauvais, and J. Tripier, Nucl. Phys. A 163, 583 (1971).
- [23] A. Prokofiev, Nucl. Instr. Meth. Phys. A 463, 557 (2001).
- [24] A.A. Kotov, et al., Phys. Rev. C 74, 034605 (2006).
- [25] R. Brandt, et al. Revue de Physique Appliquee 7, 243 (1972).
- [26] V.A. Konshin, E.S. Matushevitch, V.I. Regushevskii, Journ.: Soviet Journal of Nuclear Physics 2, 489 (1965)
- [27] G.N. Flerov, V.P. Perelygin, O. Otgonsuren, Soviet Atomic Energy 33, 1144 (1972)
- [28] Z. Todorovic, R. Antanasijevic, M. Juric, Zeitschrift fuer Physik 261, 329 (1973); E. Hagebo, T. Lund, J. Inorg. Nucl. Chem. 37, 1569 (1975); H.A. Khan, and N.A. Khan, Phys. Rev. C 29, 2199 (1984); M.C. Duijvestijn, et al., Phys. Rev. C 59,776 (1999).
- [29] R.G. Vasil'kov, and V.I. Yurevich, ICANS-XI, KEK, 1990, p.340
- [30] G. S. Bauer, Nucl. Instr. Meth. Phys. A 463, 505 (2001).
- [31] M. Zamani, S. Stoulos, M. Fragopoulou and M. Krivopustov, Phys. Rev. C87 067602 (2013)